Fresenius J Anal Chem (1997) 359 : 15–22

LECTURE

Matthias Rothmund · Armin Schütz · Andreas Brecht
Günter Gauglitz · Günther Berthel · Dieter Gräfe

Label free binding assay with spectroscopic detection for pharmaceutical screening

Received: 26 November 1996 / Revised: 17 February 1997 / Accepted: 22 February 1997

Abstract Many therapeutic drugs exert their effects by interaction with well defined molecular targets. Increasing knowledge in molecular biology allows identification of more and more molecular key compounds and in consequence a molecular approach to disease and therapy. As binding of drugs to their target compounds is a key event, binding assays with an appropriate target molecule are useful means for primary screening of novel substances. We have investigated the potential of thin film interference spectroscopy (RIFS) as a label free detection method for pharmaceutical screening in a binding inhibition assay. To meet the throughput requirements in pharmaceutical screening a parallel detection system based on imaging spectroscopy was constructed. Thrombin/thrombin inhibitor interaction was investigated as a model system. The thin film transducer was covalently modified with a thrombin inhibitor. Specific binding of thrombin and binding inhibition by inhibitor compounds could be observed. A test cycle of less than 10 min could be reached. The parallel setup allows the simultaneous detection of 96 binding curves and can reach a throughput of more than 10^6 samples per year.

Introduction

Recently, molecular fundamentals of many biochemical processes in living organisms have been at least conceptually understood which has a strong impact on the understanding and the therapy of disease and metabolic disorders. The identification of the primary molecular event of a disease or the mechanisms by which parasitic organisms attack and damage higher organisms allows a molecular approach to therapeutic drug selection and design.

M. Rothmund (✉) · A. Schütz · A. Brecht · G. Gauglitz
Institut für Physikalische Chemie, Auf der Morgenstelle 8,
D-72076 Tübingen, Germany

G. Berthel · D. Gräfe
Carl Zeiss Jena, Tatzendpromenade 1a, D-07740 Jena, Germany

Huge numbers of compounds are available from large substance stocks accumulated in pharmaceutical companies, from commercial libraries of natural or synthetic compounds [1] or from automated and combinatorial synthesis [2, 3] and can be screened using systems that allow high sample throughput. Typical test systems are cellular-based assays or tests on the molecular level, based either on variations of catalytic activity (for enzymes) or on simple binding events.

Binding assays report on the very first step involved in biological activity of a compound and are a prominent tool in drug search. Typically assays involve labels, e.g. radioisotopes (scintillation proximity assay [4], receptor binding filtration assay [5]) or fluorophores (fluorescence polarisation binding assay [6], fluorescence correlation spectroscopy [7]). The introduction of a label increases assay costs and may affect biological activity of the compounds investigated. In recent years, tools for fundamental research have emerged that allow the label free monitoring of biomolecular interaction [8]. Optical techniques are prominent in that field [9] and several systems are commercially available. Throughput requirements in drug screening are 100 000 samples per month and above. A major issue is to increase the throughput of label free detection systems to match this figure. For heterogeneous phase assays, involving immobilised reactants, the minimum assay times are set by diffusional transport of reactants. Increased throughput therefore requires parallelisation of the detection system.

Table 1 Target specifications for label free screening system

Parameter	Value
Limit of detection	< 1% of protein monolayer
Time resolution	10 s
Test cycle	10 min
Consumption of target/test	1–10 μg
Consumption of substance/test	< 1 μg
Sample positions	96

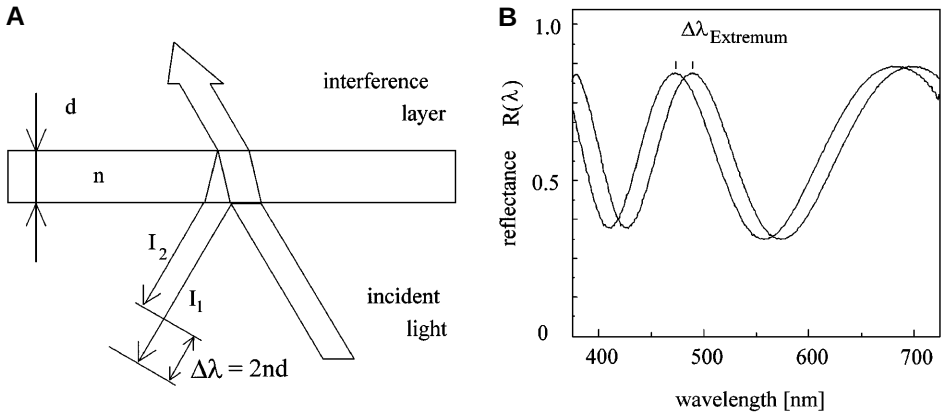

Fig. 1A, B Principle of the detection of thin layer thickness variations by reflectometric interference spectroscopy (RIFS)

We have investigated label free optical detection systems for biospecific binding events in recent years [10, 11, 12]. We have selected one approach – white light interference at thin films (RIFS) – as an especially promising tool for parallel binding assays in high throughput screening. We have set up a system realising parallel and label free readout of binding processes by imaging spectroscopy. The target specifications defined for the detection system are given in Table 1.

In this study we report on the basic performance data of the experimental setup and first results from a model receptor ligand system.

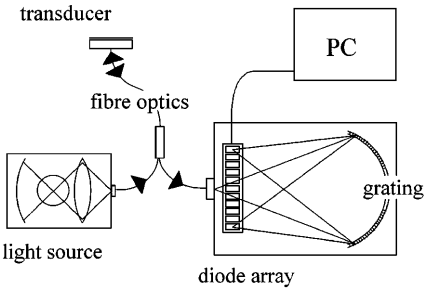

Fig. 2 Typical setup for a single channel RIFS system. White light from the light source is guided by a waveguide to the sensor plate. The reflected signal is collected by the same fiber and led to the diode-line simultaneous spectrometer. The readout is transmitted to a computer, where the thickness is evaluated continuously

Materials and methods

Transducer principle

White light interference at thin films can be used to quantify small changes in the thickness of thin transparent films. This allows the detection of protein binding effects as observed in label free binding assays. Reflectometric interference spectroscopy (RIFS, [10]) is a detection method based on thin film interference. It is based on the spectral distribution of reflectance from thin transparent layers on a glass substrate (Fig. 1). The partial beams reflected at each layer interface interfere producing a distinct reflectance pattern with alternating maxima and minima of reflectance due to constructive and destructive interference of the reflected radiation. This is expressed by:

$$R(\lambda) = I_1 + I_2 + 2\sqrt{I_1 I_2}\cos\left(\frac{4\pi nd}{\lambda}\right) \quad (1)$$

where the I_i are the intensities as shown in Fig. 1 and nd the optical pathlength, the product of refractive index n and layer thickness d. Choosing appropriate dielectric inter-layers between glass substrate and the sensing layer on the top, the reflectance signal can be optimised [13]. From this pattern the thickness of the film can be derived. Binding processes at the surface lead to an increase of the optical pathlength followed by a shift of extrema $\Delta\lambda_{Extremum}$ in the reflectance spectrum. Using numerical methods, the variation of film thickness is calculated out of the shift of the extrema in the spectrum. By single channel setups thickness variations down to a few pm can be resolved, which correspond to less than 1‰ of a protein monolayer [14].

A convenient setup for time resolved monitoring of binding events at thin interference films is based on fiber optics and diode array detectors (Fig. 2). This setup is highly effective for investigations in biomolecular interaction, but the possibilities for increasing the channel count are limited.

Parallel detection system

The parallelisation of the standard fiber optic RIFS setup would result in a complex system and a linear increase of hardware requirements and costs with detection sites. In contrast, paralleling by imaging spectroscopy techniques leads to a more simple and effective design. Imaging devices allow to monitor simultaneously discrete locations on a given transducer area with a CCD-detector. However, the properties of color CCD cameras which give access to not more than three colors are far from the requirements of RIFS measurements. An additional element is required, which allows to select small spectral bands with high reproducibility, for the assessment of spectral reflectance patterns. We have selected a fast tunable filter for this purpose, which scans a range of wavelengths sequentially. Frames are acquired by a CCD detector at each wavelength. After one wavelength scan a reflectance spectrum can be reconstructed for each CCD pixel.

Hardware components

The following construction (Fig. 3) results from the considerations given above. Starting from the light source (1) the light is collimated by the condenser (2) and passes the Lyot type tunable filter (3). A telescope lens system (4) expands the beam to the cross section area of the transducer plate (5a). A glass wedge (5) removes first surface reflections from the transducer plate mount. On top of the glass wedge a transducer chip with a thin interference layer coated on a planar glass substrate is placed. Reflections from the interference film occur at both interfaces of the film which introduces a pathlength difference of a few 100 nm thus causing interference in this range. The reflected and modulated beam is imaged by the objective lens (7) to the CCD chip. Camera and monochromator actions are controlled by a PC which also reads out camera data and calculates thickness changes. Sample handling is done by

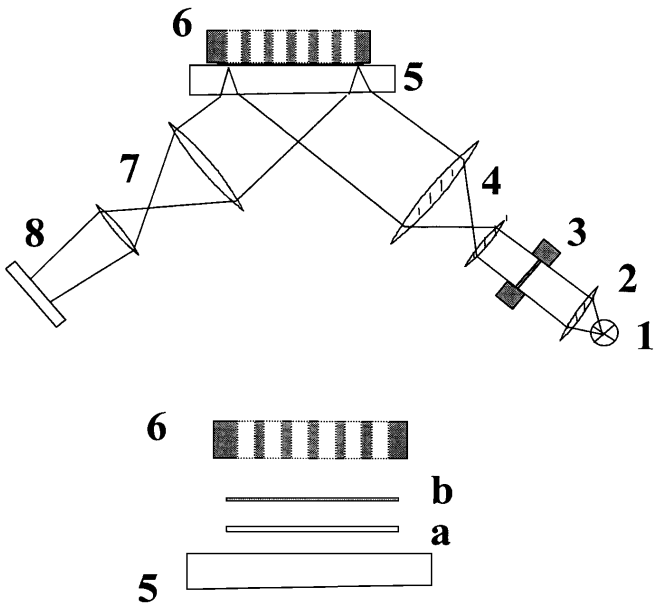

Fig. 3 Schematic view of the parallel RIFS imaging spectrometer. 1: Light source; 2: condenser lens; 3: Lyot type tunable monochromator; 4: telescope; 5: glass wedge; 6: sample plate with array of holes; 7: objective lenses; 8: CCD chip. Details a: coated glass substrate with interference layer on top; b: silicone rubber seal

pipetting from the top. The sensor area is partitioned using an appropriate seal (5b) and a sample plate (6) with an array of holes which define sample compartments.

For the construction of the parallel RIFS imaging spectrometer the commercially available components as listed in Table 2 were used.

Receptor-ligand model system and test format

The protease thrombin, a part of the coagulation system of vertebrates, and a non-peptide low molecular weight thrombin inhibitor were used as a model receptor-ligand system. Both were kindly made available by BASF Ludwigshafen. All solutions were prepared in 10 mmol L^{-1} phosphate buffered saline pH 7.4. 400 μg mL^{-1} ovalbumin were added to each sample to prevent loss of thrombin due to adsorption to walls of labware used.

A binding inhibition assay at heterogeneous phase transducers was used for detection of inhibitors. This requires the immobilisation of a reference compound to the sensor surface. Chemical modification of the sensor surface was required to allow covalent coupling and to reduce non-specific binding of test compounds, which can not be discriminated from specific binding effects. The first step consists of a treatment of the silica surface with ω-aminobutyldimethylethoxysilane, the introduction of carboxy groups by succinic anhydrid treatment and the coupling of amino dextran by carbodiimide chemistry. In a second step the carboxy groups were introduced by glutaric anhydrid treatment and a thrombin inhibitor with a free amino group was covalently linked by carbodiimide chemistry. This protocol described by Piehler et al. [15] was employed for sensor plates for the single channel setup (dimension of 10×10 mm^2) as well as for the parallel setup (60×45 mm^2).

Binding of thrombin to the transducer was tested for concentrations from 0 to 100 μg mL^{-1} for a time interval of 300 s. For the binding inhibition assay 5 μg mL^{-1} thrombin was pre-incubated with inhibitor concentrations from 0 to 1 μg mL^{-1} for 10 min. This corresponds to a 10 fold molar excess of inhibitor over thrombin. After settlement of equilibrium the modified sensor surface was exposed to the solution. Binding curves were recorded for 300 s. The surface was regenerated by 0.1 mol L^{-1} HCl. Samples were introduced to the sample cavities by manual pipetting.

Results and discussion

Optical setup

The overall system performance is critically determined by the individual components used. For optimisation of

Table 2 Components used for the parallel imaging RIFS setup

Component	Features	Type, manufacturer
Light source	100 W Halogen, microscope housing	HAL 100, Zeiss, Germany
Power supply for light source	300 W max, stability: 0.05%	Radiometric Power Supply Model 68831, LOT, Germany
Monochromator	Working principle: Liquid crystal based Lyot type filter, tuning range: 425–750 nm, FWHM: 10 nm, response time < 100 ms, wavelength-reproducibility 0.07 %	Varispec Tunable Filter, Cambridge Research and Instrumentation, USA
Optics	All components standard parts, housing as prototype	Zeiss, Germany
Sensor element	Glass substrate with dielectric coating: (Ta_2O_5 – 20 nm, SiO_2 – 375 nm) and biospecific surface modification	Schott, Germany Surface modifications according to [15]
Detection system	256×256 pixel CCD chip, 4×4 mm^2, 12 bit, 112 Hz max. framerate, 16 MB/s data rate	CA-D1-256 T, DALSA Inc, Canada
Acquisition system	PCI slot card, 40 MHz clock frequency, 4 MB on board, direct access to host main memory, controlling of the camera	ITEX IC-PCI with AM-DIG 24 T Module, Imaging Technology, USA
Evaluation system	Pentium processor, 100 MHz, PCI bus, 32 MB RAM	Board “Zappa” type, Intel, USA
Software	Prototype, source code in C, Microsoft Visual C/C++ V. 1.52/Windows 95 environment	IPC University Tübingen, Germany

working parameters and settings we have characterised the performance of the CCD camera and the spectral characteristics of the setup individually. With optimised settings the performance of the system in thickness measurements was investigated. The performance of the CCD detector is limited by drift, signal-to-noise-ratio (SNR) and the dark current offset. The drift is primarily temperature induced and negligible with the camera in thermal equilibrium. The SNR of a digital camera is mainly determined by the greatest one of the following random noise sources: 1) either the noise by limited number of discrete levels in the digitised output signal; 2) the CCD readout-noise of a single pixel; or 3) the noise of the varying number of released electrons at each pixel obeying Poisson's statistics.

The primary signal is digitised at 12 bit resolution by the camera used. Consequently the digitising noise (1) amounts to $1{:}2^{12}$, i.e. 1:4096. The (2) readout-noise of a single pixel is specified by the manufacturer as 4 DN (i.e., Digital Numbers) resulting in a dynamic range of 1:1024. For processes such as releasing charge carriers by photons in a bulk material (3) Poisson statistics is the best model to describe the resulting noise for which a high number of possible events (number of electrons released up to 10^5) and a small number of measurement cycles (number of pictures taken) is supposed. Due to the dependence of the error $\sigma = 1/\sqrt{N_{max}}$ we get for the uncertainty of the number of released electrons the square root of the maximum number of released electrons N_{max} of a single pixel, given by the manufacturer with N_{max} = 150 000. The expected noise levels are about 1:390, i.e. a value exceeding the noise levels introduced by pixel readout or digitising of the signal. The noise level under saturating conditions was measured with no light exposure at high integration times (100 ms). Under these conditions the signal is caused only by the spontaneous (thermal) generation of charge carriers and no additional noise from a light source perturbs the signal. The Poisson noise was calculated as the standard deviation of the signal distribution found for single pixels during 256 consecutively acquired frames. In good agreement with theory, this resulted in a noise level of about 1:400, i.e. about 10 DN.

Comparing these three noise sources leads to the result that the camera is dominated by Poisson noise above 5 to 10 ms integration time. Under saturating conditions, the camera delivers therefore a signal accuracy of not better than 9 bit. In Fig. 4 the dark noise (A) and the dark current (B) are shown. It is remarkable that the dark noise and dark current are starting to leave their baselines with integration times above 5 to 10 ms.

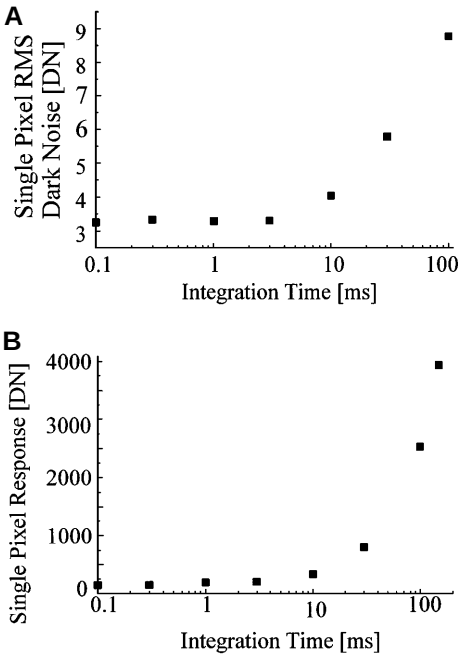

Fig. 4A, B Dark signal of the CCD camera. **A** Noise of a single pixel selected randomly; **B** Dark current of this pixel. Camera saturation value is 4095

Spectral performance

The components used in the optical part of the imaging setup show wavelength-dependent transmission or response behavior. As the performance (transmission) of lenses shows no pronounced change over this wavelength range, these need no further consideration. The transmission curve of the monochromator and the responsitivity of the camera (Fig. 5A) show decreasing performance with shorter wavelengths. As both components operate sequentially, the resulting spectral performance is given by the product of both curves (Fig. 5B). This shows that measurements at higher wavelengths are preferable. The spectral response can be flattened or extended to shorter wavelengths by use of a light source, emphasising the blue range. We have used an incandescent source with maximum emission around 600 nm. Selecting a 375 nm SiO_2 layer leads to a minimum of the reflectance curve at about 600 nm, which allows operation of the setup under good conditions.

Data reduction and time resolution

Significant amounts of raw data have to be transferred from the CCD detector during a single spectral scan. From these raw data reflectance curves are calculated for a set of discrete spots (for example 96 locations in a standard microtiterplate format). Subsequently, layer thickness at each of the spots must be calculated from the individual reflectance curves. The data evaluation strategy must match the hardware resources available. The large quantity of raw data accumulated are given in Table 3.

The amount of raw data given here can be handled within the main memory of standard PC systems. However, as in the recording of binding curves spectral scans are repeated periodically, real time reduction of the data sets is required. This is achieved in several distinct steps. Frames are accumulated continuously during acquisition.

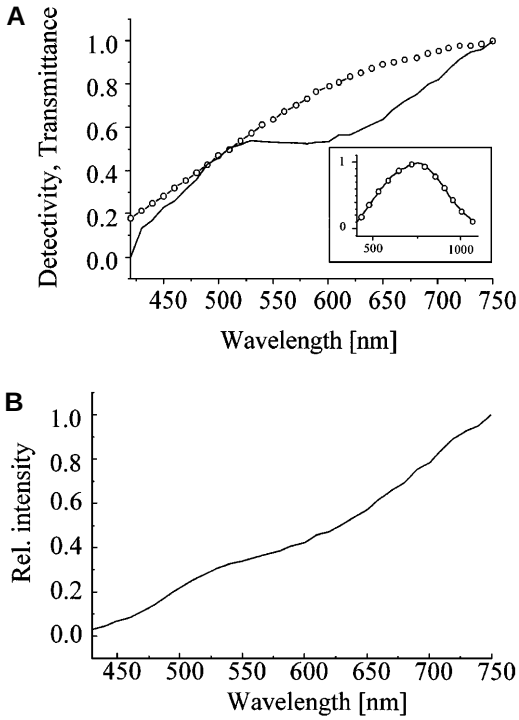

Fig. 5 **A** ○-○-: Detectivity of the CCD chip. —: Transmittance of the Lyot type monochromator. Both curves are normalised to 1. The inlay shows the CCD detectivity in overview from 500 to 1000 nm. **B** Product of detectivity and transmittance curves

Table 3 Raw data sampled for a single typical spectral scan

Procedural step	Multiplier	Raw data amount
Single frame ($256 \times 256 \times 12$ bit)	1	130 Kbytes
Oversampling at each wavelength	20 frames per wavelength	2600 Kbytes
Spectral scan at multiple wavelengths	10 wavelengths	26000 Kbytes

This reduces the amount of memory required to 260 Kbytes of buffer area (4 byte length). The time required for adjustment of the filter to a new wavelength is about 100 ms. During this time period all pixel values assigned to an individual sample area are summed, reducing the amount of data to 96 accumulated signal values per wavelength. As memory requirements are modest, these values can be stored until a full binding curve has been recorded. From the figures given above, the time per wavelength scan (10 wavelengths, 20 frames oversampling per wavelength at 30 ms per frame, 100 ms adjustment time of filter) can be estimated to about less than 10 s. Practical values were 15 s due to computation time and synchronisation requirements. Over a period of 300 s about 20 thickness values can be recorded, in order to qualify and quantify a binding curve. Currently, the sampling rate is limited by the large integration times (about 30 ms) needed because of low general light intensities and by the calculation time of the frame accumulating process. The final thickness calculation requires about 5 s plain computing time. This results in a sample throughput of 96 samples within 6 to 10 min.

Thickness resolution

A typical thickness baseline is shown in Fig. 6.

At least part of the noise sources in the overall system are of statistical nature. Random errors – like the statistical noise of the camera – can be reduced by a factor of $\sqrt{N}$ with an increase of the redundant measurements N, for example the number of pixels evaluated per sample position or the number of frames acquired per wavelength. The influence of these parameters was tested by systematic variation of the number of pixels evaluated and by varying the number of frames acquired per wavelength. The rms (root mean square) noise of at least 100 consecutive thickness readings was calculated as a noise parameter. The rms noise values were determined as the root of the mean square error of thickness readings after subtraction of any linear drift.

Measurements were carried out with the transducer element exposed to air instead of water covering the transducer element to ensure stable and consistent measurement conditions. Therefore the reflectance signal was higher and the thickness variation results were more favorable than under real conditions. Time resolution was about 10 to 15 s. The thickness variation was calculated (Fig. 6). As basic settings we evaluated about 600 pixels per sample position, acquired 20 frames per wavelength at 10 different wavelengths. In our investigation one out of these three parameters was varied.

In Fig. 7 the rms-noise of the thickness reading is given as a function of the number of pixels evaluated per detection spot. For convenience the number of evaluated pixels is given as $1/\sqrt{N}$. As expected, the thickness noise is reduced by increased N. However, the decrease of the noise with increasing number of pixels is non linear, approaching a nonzero treshold value at values below 0.2 (25 pixels and above). This indicates noise independent of the camera system. Both the light source and the Lyot type filter may contribute to the noise level found. Improvement of the noise behavior of these components may lead to noise levels below those found for about 25 pixels per location.

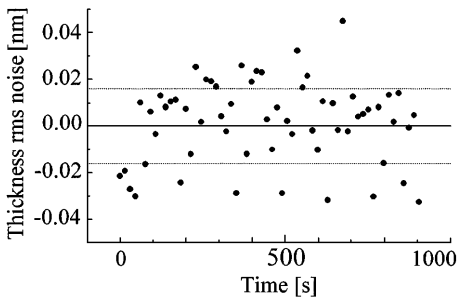

Fig. 6 Typical thickness baseline recording of a single sensor position with time interval of about 15 s. ●: Measured values. ····: Noise (standard deviation) values of about 17.9 pm

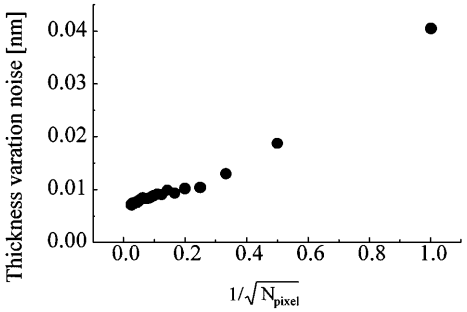

Fig. 7 Thickness noise in dependence of the number of pixels evaluated per sample position

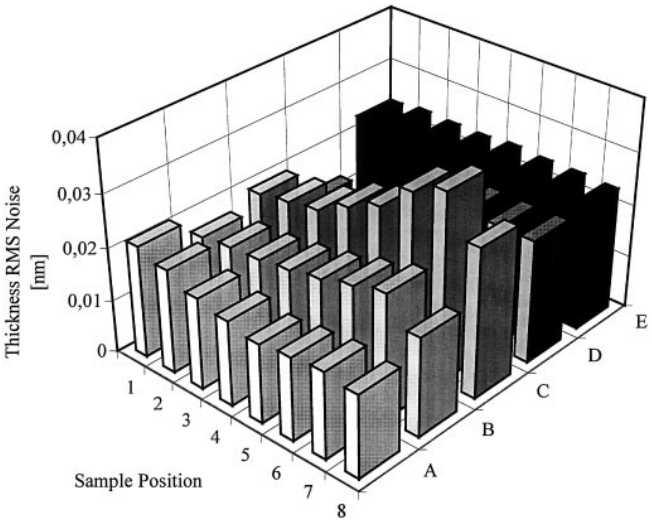

Fig. 8 Thickness rms noise at each sample position. The higher values in the "C" row are due to weaker light intensity in that region

Noise introduced by fluctuations of the monochromator system and the light source can be reduced by frame-oversampling. Noise levels found vary from about 75 pm ± 12 pm found for 1 frame per wavelength down to 14 pm ± 3 pm for 36 frames sampled per wavelength. A number of 600 pixels was evaluated for this measurement.

Thickness rms-(root-mean-square)-noise levels of 10 to 20 pm can be achieved under reasonable conditions (25 frames oversampling; 100 pixels). It is important to notice that 100 pixels represent less than 0.5% of the total CCD chip area.

As a final result of our measurements thickness resolution of an area of the sample array is shown in Fig. 8. This shows that the distribution of noise values is homogeneous, with small deviations introduced by imperfections of the illuminating system. This also is a point for further improvement.

Affinity detection

The single channel setup (Fig. 2) was used to prove the feasibility of a non-stirred system for affinity detection.

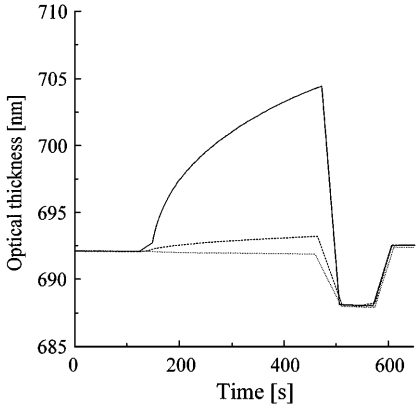

Fig. 9 Characterisation of the sensor surface. Binding of two different thrombin concentrations 10 µg mL^{-1} (---) and 100 µg mL^{-1} (—) were determined in a single channel setup. The non-specific binding was tested with 400 µg mL^{-1} ovalbumin (····). The drop at t = 500 s is due to regeneration of the surface at low pH values

Thrombin and a low molecular weight thrombin inhibitor were used as a model receptor-ligand-system.

The modified sensor surfaces were characterised with two different thrombin concentrations 10 and 100 µg mL^{-1}, respectively (Fig. 9). The increase of the optical thickness by binding on the surface depends on the thrombin concentration. As shown in Fig. 9 the non-specific binding of ovalbumin in high concentration at the amino dextran layer is negligible.

Linear relation between the change of optical thickness and the thrombin concentration from 0 to 10 µg mL^{-1} was found. A signal change of about 300 pm at a thrombin concentration of 5 µg mL^{-1} after 300 s was detected by the diffusion controlled binding of thrombin in the non-stirred system (data not shown). The noise level found for the system (app. 20 pm rms) sets a limit of detection (3s) of at least 60 pm thickness change. Therefore signal levels of a few 100 pm allow unambiguous detection of binding events.

Screening applications require the detection of potential therapeutic agents out of large substance libraries. The detection system presented here allows to identify substances with affinity for the active site of thrombin by inhibition of thrombin binding at the transducer surface. The feasibility of a binding inhibition assay was tested with a non-peptide thrombin inhibitor supplied by BASF. In this assay free thrombin and the inhibitor are pre-incubated and the amount of free thrombin in equilibrium is determined by exposing the sensor element to the sample mixture. The change of the optical thickness by thrombin binding on the surface decreases with increasing concentration of the added inhibitor (Fig. 10).

Protein binding in the parallel detection system was tested by recording the binding of thrombin on the modified sensor element (Fig. 11). Binding curves from the parallel setup show the same shape and the same order of magnitude of changes in optical thickness (about 1 nm in 100 s at a thrombin concentration of 100 µg mL^{-1}) com-

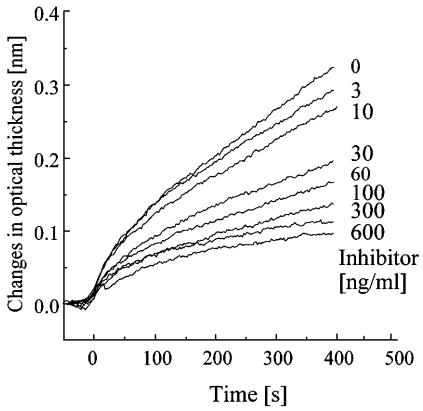

Fig. 10 Inhibition of thrombin binding by increasing concentrations of an active site inhibitor. The measurements were carried out in a single channel setup. (Thrombin concentration 5 μg mL^{-1})

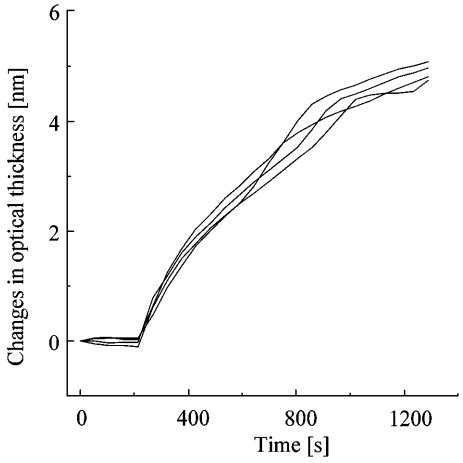

Fig. 11 Thrombin binding on a sensor surface in a parallel setup. The binding of thrombin (100 μg mL^{-1}) was measured in four wells (randomly selected) simultaneously

pared to the single channel setup. A sampling frequency of about 0.05 Hz was achieved with the parallel detection system. These results proof the feasibility of the parallel detection concept for screening applications and allow a comparison of both systems.

Summary and outlook

Our investigations show that imaging spectroscopy allows construction of a parallel system for label-free binding assays. Protein binding results in a change of the spectral reflectance properties of the transducer surface. The use of a fast tunable filter and a CCD detector allows acquisition of spatially resolved reflectance spectra with a time resolution of better than 0.05 Hz. Time resolution is limited by the tuning speed of the filter system, by the signal to noise ratio required (which may dictate oversampling), and by the throughput of the data evaluation hardware. During continuous acquisition of spectra, the PCI-bus PC system used limits throughput for 256×256 pixel frames to video frame rates (around 20 Hz). The spectral characteristics of the components used restrict operation in the red to near infrared region of the spectrum.

The optical thickness of the thin film transducer structure used for label free binding assays could be determined with a noise level of less than 20 pm. Specific binding of thrombin to a transducer modified with a thrombin inhibitor could be demonstrated in the parallel setup. The feasibility of a binding inhibition test format for the identification of tentative thrombin inhibitors was demonstrated in a single channel setup. The thickness resolution achieved in the parallel setup corresponds to a limit of detection of about 1% of a protein monolayer. This is sufficient for screening at the concentrations set as target levels for this study.

Sample compartments can be filled from the top, allowing simple interfacing to pipetting robots. The transducer concept is based on direct imaging and allows arbitrary partitioning of the sample area, allowing increased throughput of the system by reducing the size of the individual sample area. Another benefit of miniaturised sample areas will be a reduced consumption of test materials. Active areas far below 1 mm^2 are possible. Large transducer areas with high sample count can be addressed by CCD transducers with high pixel numbers (CCDs with 10^6 pixels are currently available), but dedicated processing boards for data reduction with high bandwidth bus systems interfacing to the frame grabber hardware would then be necessary.

The concept of wavelength sequential imaging spectroscopy was successfully applied to a bioanalytical problem. The approach is adaptable to other thin film transducer structures and other problems, where a wavelength encoded signal requires spatial readout. The results indicate that the performance of available hardware is well suited to spectroscopic imaging, when spectral and temporal resolution are not highly critical.

Acknowledgements This work was funded by the "Bundesministerium für Bildung und Forschung" (BMBF) and the Graduiertenkolleg "Identifizierung und quantitative Analyse pharmazeutisch und biochemisch relevanter Substanzen". Substances for the thrombin measurements were a kind gift of BASF Ludwigshafen, Germany.

References

1. Lebl M, Krchnak V, Sepetov N, Seligmann B, Strop P, Felder S, Lam KS (1995) Biopolymers 37:177
2. Jung G (1996) Combinatorial Peptide and Nonpeptide Libraries. VCH Verlagsgesellschaft mbH, Weinheim
3. Houghten RA, Pinilla C, Blondelle SE, Appel JR, Dooley CT, Cuervo JH (1991) Nature 354:84–86
4. Bosworth N, Towers P (1989) Nature 341:167
5. Slack J, Sims JE, Pitt AM, Dower SK (1989) BioTechniques 7: 1136–1138
6. Dandliker WB, Saussure VA de (1970) Immunochemistry 7: 799
7. Eigen M, Rigler R (1994) Proc Natl Acad Sci USA 91:5740–5747

8. Joensson U, Faegerstam L, Ivarsson B, Johnsson B, Karlsson R, Lundh K, Loefaas S, Persson B, Roos H, et al (1991) BioTechniques 11:620
9. Brecht A, Gauglitz G (1995) Biosens Bioelectronics 10:923–936
10. Gauglitz G, Brecht A, Kraus G, Nahm W (1993) Sens Actuators B11:21
11. Striebel C, Brecht A, Gauglitz G (1994) Biosens Bioelectronics 9:139
12. Drapp B, Piehler J, Brecht A, Gauglitz G, Luff BJ, Wilkinson JS, Ingenhoff J (1997) Sens Actuators B (in press)
13. Brecht A, Gauglitz G (1994) Fresenius J Anal Chem 349:360–366
14. Piehler J, Brecht A, Gauglitz G (1996) Anal Chem 68:139–143
15. Piehler J, Brecht A, Geckeler KE, Gauglitz G (1996) Biosens Bioelectronics 11:579–590